

Supplementary Information

Compact high-quality CdSe/CdS core/shell nanocrystals with narrow emission linewidths and suppressed blinking

Ou Chen¹, Jing Zhao¹, Vikash P. Chauhan², Jian Cui¹, Cliff Wong¹, Daniel K. Harris¹, He Wei¹, Hee-Sun Han¹, Dai Fukumura², Rakesh K. Jain² and Mouni G. Bawendi^{1*}

¹ Department of Chemistry, Massachusetts Institute of Technology, 77 Massachusetts Ave., Cambridge MA 02139 (USA)

² Massachusetts General Hospital and Harvard Medical School, 100 Blossom St., Boston, MA 02114 (USA)

* e-mail: mgb@mit.edu

Chemicals

1-octadecene (ODE, 90%), trioctylphosphine oxide (TOPO 99%), trioctylphosphine (TOP, 97%), oleylamine (OAm, 70%), 1-octanethiol (> 98.5%), selenium dioxide (SeO₂, 99.9+%), sulphur powder (99.999%) and poly(methyl methacrylate) (PMMA, 350k MW) were obtained from Aldrich. Cadmium oxide (CdO, 99.998%), cadmium nitrate tetrahydrate (Cd(NO₃)₂·4H₂O, 99.99%), selenium powder (99.999%), myristic acid (MA, 99%), oleic acid (OLA, 90%) and octadecylphosphonic acid (ODPA, 97%) were purchased from Alfa Aesar. Methoxy-polyethylene-glycol thiol PEG-SH (5000 MW) was obtained from Rapp Polymere GmbH, Tuebingen, Germany.

CdSe core synthesis

Wurtzite-CdSe (W-CdSe) cores were synthesized according to a literature method¹. Briefly, 60 mg CdO, 280 mg octadecylphosphonic acid (ODPA) and 3 g trioctylphosphine oxide (TOPO) were added to a 50 mL flask. The mixture was heated to 150 °C and degassed under vacuum for 1 hour. Under nitrogen flow, the reaction mixture was heated to 320 °C to form a colourless clear solution. After adding 1.0 mL trioctylphosphine (TOP) to the solution, the temperature was brought up to 380 °C, at which point Se/TOP (60 mg Se in 0.5 mL TOP) solution was swiftly injected into the flask. When the CdSe core nanocrystals reached the desired size, the reaction was terminated by removing the heat. The resulting CdSe particles were precipitated by adding acetone and dispersed in hexane as a stock solution.

Zinc-Blende-CdSe (ZB-CdSe) cores were synthesized via a previously described method². In general, selenium dioxide powder (0.1 mmol) and cadmium myristate (0.1 mmol) were added to a three-neck flask with ODE (5.0 g). The mixture was degassed for 10 min under vacuum at room temperature. Under argon flow, the solution was stirred and heated to 240 °C at a rate of 25 °C/min. After 2 minutes of growth, 0.1 mL of oleic acid was added dropwise into the reaction solution to stabilize the growth of the nanocrystals. The reaction was monitored by UV-Vis spectroscopy and was stopped by removing the heat when the nanoparticles reached a desired size. The resulting particles were precipitated by adding acetone, and then redispersed in hexane as a stock solution.

CdS shell growth

For the shell growth reaction, a hexane solution containing 100 nmol of CdSe QDs was loaded in a mixture of 1-octadecene (ODE, 3 mL) and oleylamine (OAm, 3 mL). The reaction solution was degassed under vacuum at room temperature for 1 hour and 120 °C for 20 min to completely remove the hexane, water and oxygen inside the reaction solution. After that the reaction solution was heated up to 310 °C with a heating rate of 18 °C/min under nitrogen flow and magnetic stirring. During the heating, when the temperature reached 240 °C, a desired amount of cadmium (II) oleate (Cd-oleate, diluted in 6 mL ODE) and octanethiol (1.2 equivalent amounts refer to Cd-oleate, diluted in 6 mL ODE) began to be injected dropwise into the growth solution at a rate of 3 mL/hr using a syringe pump. After finishing precursor infusion, 1 mL oleic acid was quickly injected and the solution was further annealed at 310 °C for 60 min. The resulting CdSe/CdS core/shell QDs were precipitated by adding acetone, and then redispersed in hexane. The particles were further purified by precipitation-redispersion for two more rounds and finally suspended in ~2 ml hexane or chloroform.

Conventional shell growth reaction followed a literature method³. Briefly, a hexane solution containing 100 nmol of CdSe QDs was loaded in a mixture of 1-octadecene (ODE, 6 mL) and octadecylamine (ODA, 1.5 g). The reaction solution was degassed under vacuum at room temperature for 1 hour and 120 °C for 20 min to completely remove the hexane, water and oxygen inside the reaction solution. After that, the reaction solution was heated up to 240 °C under nitrogen flow and magnetic stirring. CdS shells were grown monolayer by monolayer, by alternate injections of Cd-oleate (0.1 M in ODE) and sulphur (0.1 M in ODE) precursors. The injection time for each monolayer was 3~5 min. The growth time was 10 min after each injection. When the desired CdS shell thickness was achieved, the growth

solution was cooled to room temperature. The resulting CdSe/CdS core/shell QDs were precipitated by adding acetone, and then redispersed in hexane. The particles were further purified by precipitation-redispersion for two more rounds and finally suspended in ~2 mL hexane or chloroform.

Polymeric imidazole ligands (PILs) synthesis

PILs synthesis followed a previous reported method⁴. Monomers are prepared by coupling primary amine bearing moieties with acrylic acid via an amide bond forming reaction. In a typical polymerization, monomers were added to an 8 mL vial. The solvent was removed in vacuo and 50 μ L of dry dimethylformamide (DMF) along with RAFT and azobisisobutyronitrile (AIBN) were added. The contents of the vial were transferred to a 1 mL ampule. The ampule was subjected to 4 cycles of freeze-pump-thaw, and sealed under vacuum using a butane torch. The vial was heated to 70 °C on an oil bath for 1.5–3 h, after which 0.5 mL of a 4 M HCl in dioxane solution was added to cleave the BOC protecting groups. After 1 h at room temperature, the HCl was removed in vacuo. The deprotected polymer was dissolved in methanol (MeOH), to which a solution of NaOH in MeOH (1M) was added dropwise to adjust the pH to be between 8–9. The solvent was removed in vacuo, and then CHCl_3 was added to precipitate the salts. The solution was filtered through a 0.45 μ m PTFE filter and the solvent removed in vacuo to yield the final polymer for QD ligand exchange.

Ligand exchange

With methoxy-polyethylene-glycol thiol (PEG-SH): The CdSe/CdS core/shell QD (either conventional (conv.) QDs or our new generation (ng) QDs with the same CdSe core diameter of 4.4 nm and CdS shell thickness of 2.3 nm) solution (1nmol in 100 μ L chloroform) was added to a freshly prepared chloroform solution of PEG-SH (65 mg in 100 μ L) placed in a septum-capped 8 mL vial. 20 μ L of 15 nM NaBH_4 in methanol were added. The final mixture was stirred at room temperature for ~15 hr. The final solution was diluted with 100 μ L of chloroform and the QDs were precipitated by adding hexanes. After 2 min of centrifugation at 3000 rcf, the supernatant was discarded and the QDs were dissolved in 200 μ L of methanol. The methanol was removed by vacuum and 1X PBS (3 mL) was then added. The core/shell QD solution was filtered through a 0.2 μ m syringe filter, dialyzed in a centrifugation filter (3,000 MW cut off, cellulose, Millipore), filtered once more through a 100 nm centrifugation filter and stored at 4 °C.

With polymeric imidazole ligands (PILs): The ng CdSe/CdS core/shell QDs (CdSe core diameter of 4.4 nm and CdS shell thickness of 2.3 nm) solution (1nmol in 100 μ L chloroform) was added to a chloroform solution of PILs (5 mg in 100 μ L) placed in a septum-capped 8 mL vial. The solution mixture was stirred at room temperature for \sim 20 min, after which 30 μ L of methanol was added, followed by stirring for an additional 4 hr. The final solution was diluted with 50 μ L of chloroform and 50 μ L of ethanol. The QDs were precipitated by adding hexanes. After 2 min of centrifugation at 3000rcf, the supernatant was discarded and the QDs were dissolved in 200 μ L of methanol. The methanol was removed by vacuum and 1X PBS (3 mL) was then added. The core/shell QD solution was filtered through a 0.2 μ m syringe filter, dialyzed in a centrifugation filter (3,000 MW cut off, cellulose, Millipore), filtered once more through a 100 nm centrifugation filter and stored at 4 °C.

Samples for ^1H -NMR measurements

Reaction without the addition of Cd-oleate: A hexane solution containing 100 nmol of CdSe QDs was loaded in a mixture of 1-octadecene (ODE, 0.5 mL) and oleylamine (OAm, 0.5 mL). The reaction solution was degassed under vacuum at room temperature for 1 hour and 120 °C for 20 min to completely remove the hexane, water and oxygen inside the reaction solution. After that, the reaction solution was heated up to 310 °C with a heating rate of 18 °C/min under nitrogen flow and magnetic stirring. When the temperature reached 240 °C, 50 μ L octanethiol (diluted in 150 μ L ODE) was slowly injected in the reaction solution. The reaction solution kept at 310 °C for 30 min and then cooled down to room temperature. 10 μ L of the crude reaction solution was diluted in \sim 0.8 mL CDCl_3 for ^1H -NMR measurement. NMR spectra were measured on a Varian Inova 500 MHz spectrometer at ambient temperature and referenced to internal ^1H solvent peaks.

Reaction with the addition of Cd-oleate: The procedure is identical to the reaction without the addition of Cd-oleate described above, except that 50 μ L octanethiol (diluted in 150 μ L ODE) and Cd-oleate (1.44 mL, 0.2 M in ODE) were simultaneously injected in the reaction solution. 10 μ L of the crude solution was diluted in \sim 0.8 mL CDCl_3 for ^1H -NMR measurement.

Photon correlation Fourier spectroscopy in solution (S-PCFS) measurement

Photon-correlation Fourier spectroscopy (PCFS) is a method for extracting fast timescale spectral information from single emitters. Combining a Michelson interferometer with a Hanbury Brown and Twiss correlation setup, the intensity cross-correlation function as a function of path-length difference is related by Fourier transform to the spectral correlation function^{5, 6}.

Coupled with fluorescence correlation spectroscopy (FCS), Solution PCFS (S-PCFS) can extract spectral information about the average single emitter within an ensemble in solution at timescales much faster than accessible through traditional single-particle spectroscopy with high temporal resolution, large sample sizes and without selection bias. In this arrangement, by measuring the intensity cross-correlation functions as well as the autocorrelation of the total intensity, the spectral correlation function for the average single emitter as well as the spectral correlation function for the ensemble can be measured simultaneously. Details of the experimental setup, implementation and analysis can be found in Ref. 5 and Ref. 6.

For this work, a thin flat capillary containing a dilute solution of the sample was mounted onto an inverted confocal microscope with a 1.2 NA water-immersion objective. 514 nm cw excitation was used in conjunction with a 525 nm long-pass emission filter. Samples were prepared by diluting a concentrated stock solution into hexanes containing excess cadmium oleate and decylamine to help prevent aggregation. Intensity cross-correlation and autocorrelation functions were simultaneously calculated with a digital correlator (ALV7004/FAST).

For each sample, 123 scans were measured over 81 positions. Each step of the linear stage changed the path-length difference by 1 μm covering path-length differences from -40 μm to +40 μm . The centre 21 positions were measured three times and the correlation function values at the designated time separation τ were averaged. The mirror on one arm of the interferometer was translated by a piezo actuator over a distance of ~ 2 wavelengths at a frequency of 0.05 or 0.07 Hz. The ensemble component was chosen at τ sufficiently long such that photons are no longer correlated for the single emitter. The diffusion and ensemble-corrected intensity correlation function for the single-emitter was averaged between 1-10 μs . An afterpulse correction was performed as described in Ref. 5 and Ref. 6.

The intensity correlation function as a function of path-length difference, for both the single and ensemble components, was fit to a constrained 3-Gaussian function as described in Ref. 6. This fitting function, which fits well to the data, arises from the assumption that the underlying spectrum is well-

approximated by the sum of two Gaussian functions. The full-width at half-maximum of the calculated effective spectral lineshape can be numerically calculated and reported as the linewidth.

Photoluminescence (PL) intensity trace measurement for single-QDs

For single-QD measurements, the CdSe/CdS core/shell QDs were diluted in a toluene/poly(methyl methacrylate) (PMMA) solution (4% by weight) and spun cast onto glass coverslips (Electron Microscopy Sciences). Individual QDs were studied by confocal fluorescence microscopy using an oil immersion microscope objective (100X, 1.40 NA, Plan Apochromat). The QDs were excited with a continuous wave laser at 514 nm with a power density of 80 W/cm². The emission of single NCs was divided in half using a beam splitter and focused onto two avalanche photodiodes (APDs) (Perkin-Elmer) in a Hanbury-Brown and Twiss geometry using suitable spectral filters. PL intensity time traces and $g^{(2)}(\tau)$ correlation functions were simultaneously recorded using pulse counters (National Instruments) and a correlator card (Timeharp 200, PicoQuant). All measurements were performed at room temperature. We determine the PL threshold of the “off” state through the histogram of the PL intensity. The binary separation of a bright “on” state and a dark “off” state is very clear. We also verify that small changes in the “off” threshold do not affect the “on” time fraction calculation. We made sure that our “on” time fractions were not overestimated and in practice then all the thresholds were chosen as the average background count plus at least 6 times its standard deviation.

Calculation of ensemble PL QYs evolution

The average times that a QD stays in an “on”/ “off” states can be expressed as:

$$\langle t_{on/off} \rangle = \int_{t_{min}}^{t_{acq}} t \times P_{on/off} dt / \int_{t_{min}}^{t_{acq}} P_{on/off} dt \quad (1)$$

where t_{min} is the bin time (50 ms in our study), and t_{acq} is the total acquisition time. $P_{on/off} = C t^{-\alpha_{on/off}}$, C is a constant, $\alpha_{on/off}$ are the power-law exponents characterizing the statistics of “on”/“off” events.

After mathematical transformation, Equation (1) can be expressed as:

$$\langle t_{on/off} \rangle = \frac{1-\alpha_{on/off}}{2-\alpha_{on/off}} \times \frac{t_{acq}^{(2-\alpha_{on/off})} - t_{min}^{(2-\alpha_{on/off})}}{t_{acq}^{(1-\alpha_{on/off})} - t_{min}^{(1-\alpha_{on/off})}} \quad (2)$$

The “on” time fraction f_{on} , representing the ensemble PL QY can be calculated as:

$$f_{on} = \langle t_{on} \rangle / (\langle t_{on} \rangle + \langle t_{off} \rangle) \quad (3)$$

The calculated evolution of the ensemble PL QY (“on” fraction) in time using this equation is shown in Fig. S12a.

PL intensity trace measurement for a collection of QDs

To collect the PL intensity from a collection of QDs, the QDs were spun cast from a dilute PMMA solution onto a glass coverslip. The concentration of QD solution was low enough so that the interaction between QDs is negligible in the resulting QD film. The QD film was then sandwiched between the coverslip and a cover glass with the edge sealed with Epoxy. All the sample preparation (dilution, spin-cast and packaging) was performed in a glove box under nitrogen environment. The packaged QD film was excited with a 514 nm continuous wave laser at $\sim 80 \text{ W/cm}^2$, the same power density as the single QD measurement. The laser excitation was defocused to a 50 μm diameter spot so that a collection of QDs was excited simultaneously. The emission from a collection of QDs was collected by an APD with proper spectral filters for as long as $\sim 72000 \text{ sec}$ ($\sim 20 \text{ hr}$).

Solution PL lifetime measurement

To measure the PL lifetime of an ensemble of QDs, the QDs were diluted in a hexane solution and excited at 414 nm with a 2.5 Mhz repetition rate. The emission from the QD solution was collected by an APD with appropriate spectral filters. The photon arrival time was correlated with the excitation pulse by a Timeharp 200 correlator.

Biological fluorescence imaging study

Animal models: Imaging studies were carried out in Tie2-GFP transgenic mice (FVB background)⁷ bearing dorsal skinfold chambers^{8,9}. All animal procedures were carried out following the Public Health

Service Policy on Humane Care of Laboratory Animals and approved by the Institutional Animal Care and Use Committee of the Massachusetts General Hospital.

In vivo imaging: Three sets of QDs – QD_{conv.}-SH-PEG, QD_{ng}-SH-PEG, and QD_{ng}-PIL – were prepared for intravenous injection in separate Tie2-GFP mice at identical concentrations of 2.5 μ M. Following retro-orbital injection of 200 μ L with these concentrations, multiphoton imaging was carried out as described previously¹⁰ on a custom-built multiphoton laser-scanning microscope using confocal laser-scanning microscope body (Olympus 300; Optical Analysis Corp.) and a broadband femtosecond laser source (High Performance MaiTai, Spectra-Physics). In these mice, the endothelial cells that form the lining of blood vessels express GFP and fluoresce green¹¹, while the red fluorescence from injected QDs labels the vasculature. Image slices were taken at ~60mW at the sample surface with depths from 0 - 150 μ m, 30min after injection. Imaging studies were performed with a 20X magnification, 0.95NA water immersion objective (Olympus XLUMPlanFl, 1-UB965, Optical Analysis). Image analysis was carried out using ImageJ.

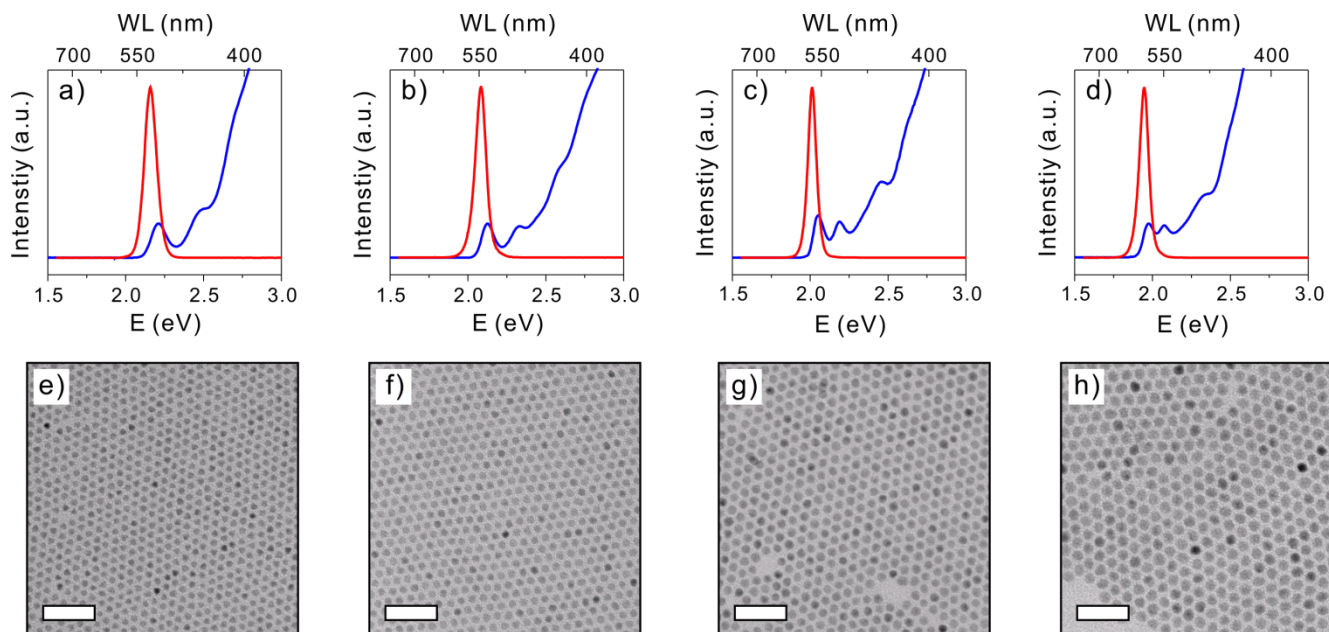


Figure S1. a)-d) Absorption (blue) and photoluminescence (PL) (red) spectra of four different CdSe/CdS core/shell QDs samples synthesized through our novel method with CdSe core diameters of a) 2.7 nm, b) 3.4 nm, c) 4.2 nm and d) 5.4 nm and CdS shell thickness of 1.85 nm, 2.1 nm, 2.0 nm and 2.3 nm. The corresponding TEM images of these four samples are shown in e)-h). Scale bars are 50 nm.

Table S1: Properties of different CdSe/CdS core/shell QDs samples.

CdSe core				CdSe/CdS core/shell				
λ_{abs} (nm)	λ_{em} (nm)	FWHM (meV/nm)	Radius (nm)	λ_{abs} (nm)	λ_{em} (nm)	FWHM (meV/nm)	shell thickness (nm)	PL QY (%)
487	503	128/~26	~1.35	563	576	93.5/~26	~1.85/~5.5ML	87
522	535	108/~25	~1.7	585	597	83.2/~24	~2.1/~6ML	90
561	571	95.2/~25	~2.1	607	618	65.3/~20	~2.0/~6ML	94
569	580	96.2/~26	~2.2	615	625	67.1/~20	~2.4/~7ML	97
605	613	80.7/~24	~2.7	631	639	67.5/~22	~2.3/~7ML	89

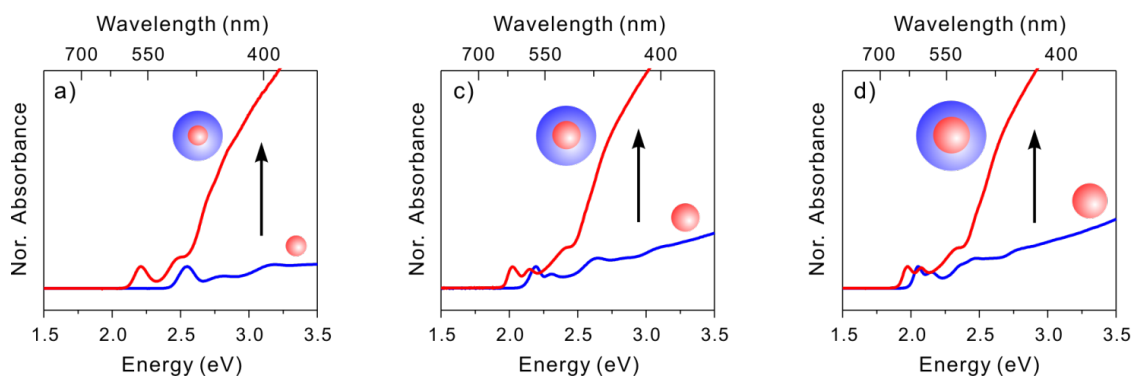


Figure S2. Absorption spectra of CdSe nanocrystal QDs (blue line) and the final CdSe/CdS core/shell nanocrystal QDs (red line) with different CdSe core diameters (a: 2.7 nm, c: 4.4 nm, d: 5.4 nm) and CdS shell thickness of 5~7 monolayer (ML). The dramatically increased absorption cross section at energies higher than the CdS band gap (2.42eV, 513nm) is consistent with the formation of the CdS shell.

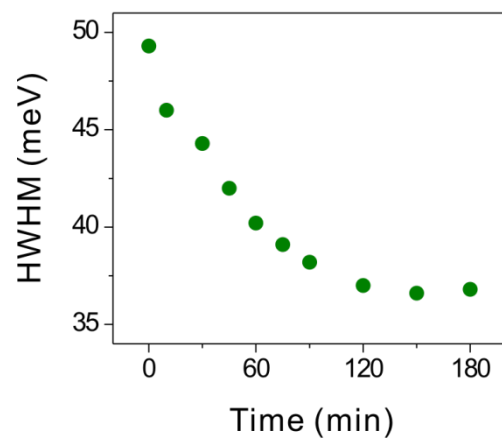


Figure S3. Half width at half maximum (HWHM) of the first absorption peak of CdSe/CdS core/shell QDs (shown in Figure 1e-h) decreased from 49.2 meV for CdSe core to 36.6 meV for final CdSe/CdS core/shell QDs during the CdS shell growth reaction.

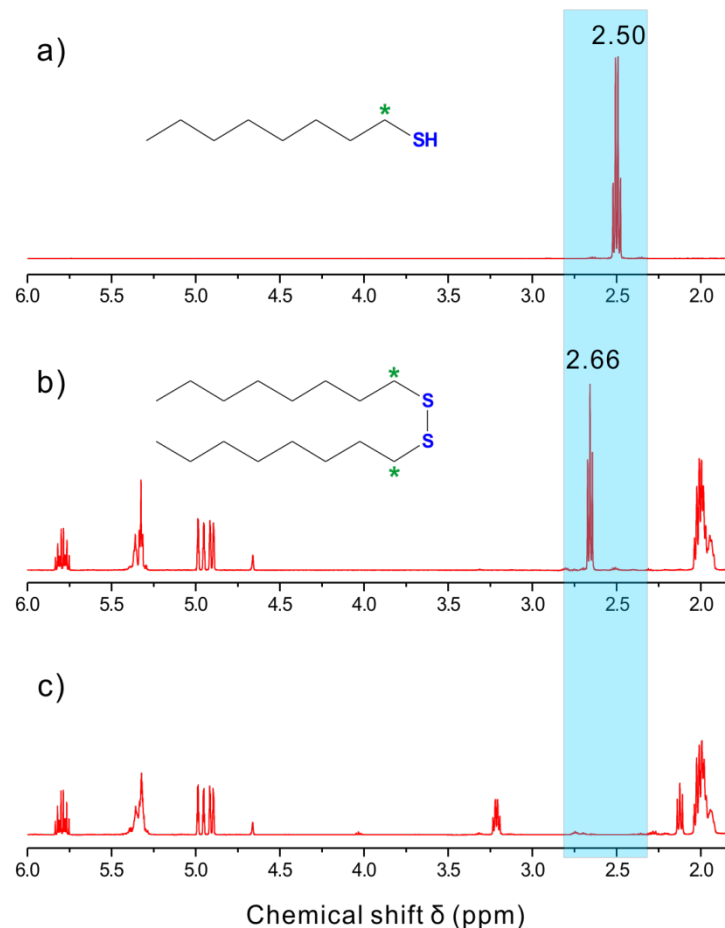


Figure S4. ^1H -NMR spectra of QD shell growth solutions demonstrate that cadmium oleate (Cd-oleate) mediates the cleavage of 1-octanethiol's carbon-sulphur bond, liberating the sulphur for formation of the CdS shell. a) ^1H -NMR of 1-octanethiol. Highlighted region shows α -hydrogen peak of 1-octanethiol at δ 2.50 (2H, dt, $J = 7.5, 7.5$ Hz), b) ^1H -NMR of shell growth solution with 1-octanethiol but without Cd-oleate results in oxidation of 1-octanethiol into di-n-octyl disulphide but not cleavage of the carbon-sulphur bond. Highlighted region shows α -hydrogen peak of di-n-octyl disulphide at δ 2.66 (4H, t, $J = 7.2$ Hz), c) ^1H -NMR of shell growth solution with 1-octanethiol and Cd-oleate results in absence of α hydrogen peaks from both octanethiol and di-n-octyl disulphide, suggesting cleavage of the carbon-sulphur bond and subsequent growth of the CdS shell as confirmed by optical, TEM, EDS and XRD analyses.

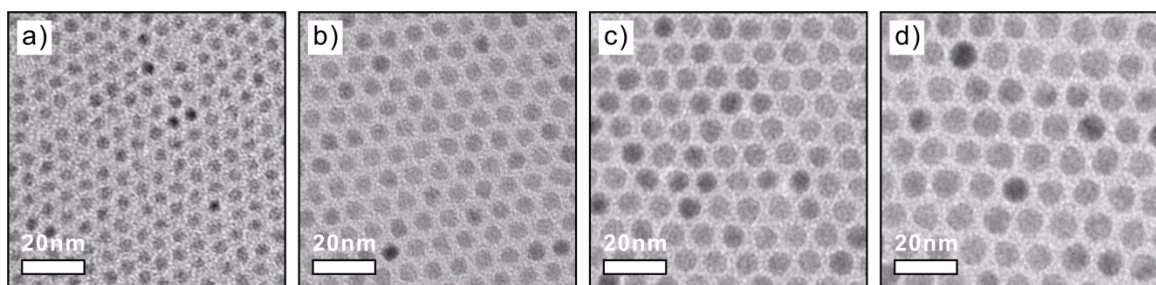


Figure S5. Zoomed-in TEM images of a) 4.4nm CdSe core and b)-d) CdSe/CdS core/shell QDs with a CdS shell thickness of 0.8nm, 1.6nm, 2.4nm, respectively.

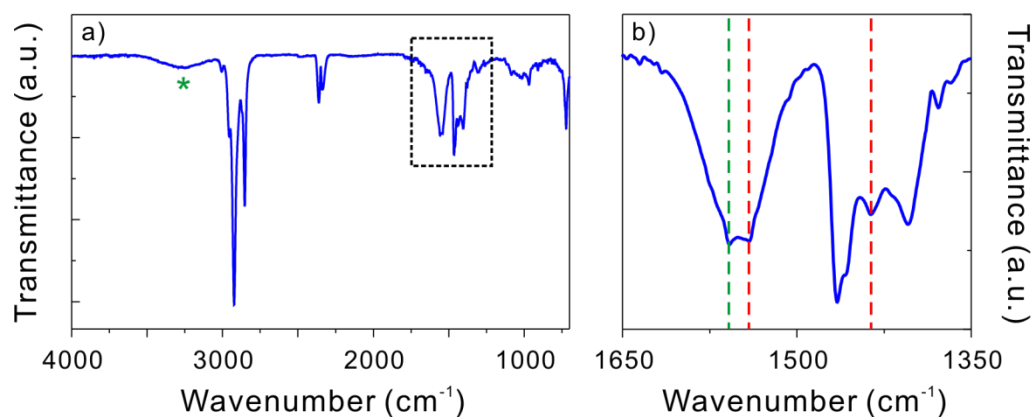


Figure S6. a) FT-IR transmittance spectrum of purified CdSe/CdS core/shell QDs synthesized by our method. b) The zoomed-in FT-IR spectrum of the highlighted area in a). The characteristic N-H bending vibration band appeared at 1558 cm^{-1} (labeled by the green dash line in panel b) and the N-H stretching vibrations emerged as the weak and broad band at the range of $3000\text{--}3300\text{ cm}^{-1}$ (labeled by the green star in panel a). The asymmetric and symmetric stretching vibrations of carboxylate group (-COO^-) appeared at 1541 cm^{-1} and 1436 cm^{-1} (labeled by the red dash lines in panel b), respectively. The FT-IR spectrum clearly shows the coexistence of OAm and oleate on these CdSe/CdS core/shell QDs surface.

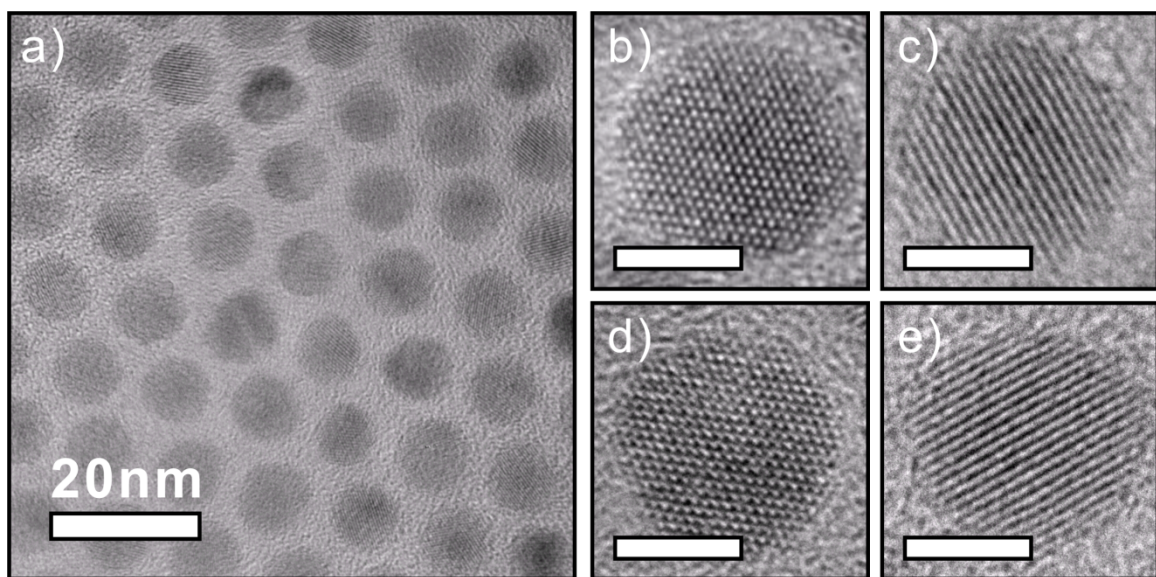


Figure S7. High-resolution TEM images of CdSe/CdS core/shell QDs, indicating high crystallinity of individual QDs. Scale bars in b)-e) are 5 nm.

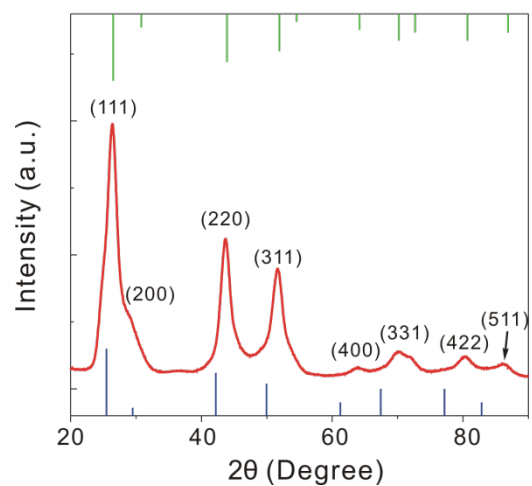


Figure S8. X-ray powder diffraction pattern of CdSe/CdS core/shell QDs with 4.0 nm diameter zinc-blende CdSe core and 2.9 nm CdS shell thickness. The stick patterns show the standard peak positions of bulk zinc-blende CdSe (bottom blue sticks) and CdS (top green sticks).

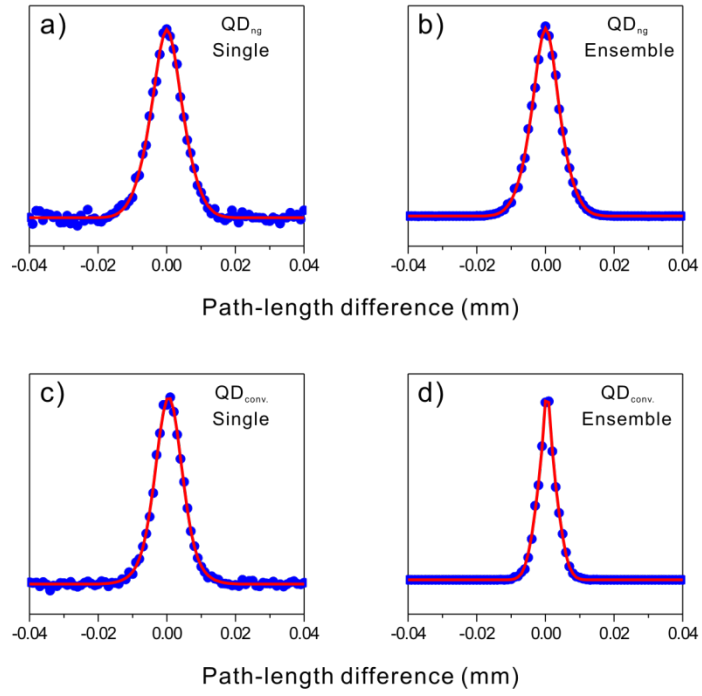


Figure S9. Blue dots are the values of the diffusion and ensemble-intensity correlation functions as a function of path-length difference for a) single new generation (ng) QDs (QD_{ng}) synthesized with our method and c) single conventional QDs ($QD_{conv.}$) synthesized through the literature method³. Correlation function values for the ensemble are shown in b) for our new method and d) for the conventional method. Red lines are the corresponding 3-Gaussian fits.

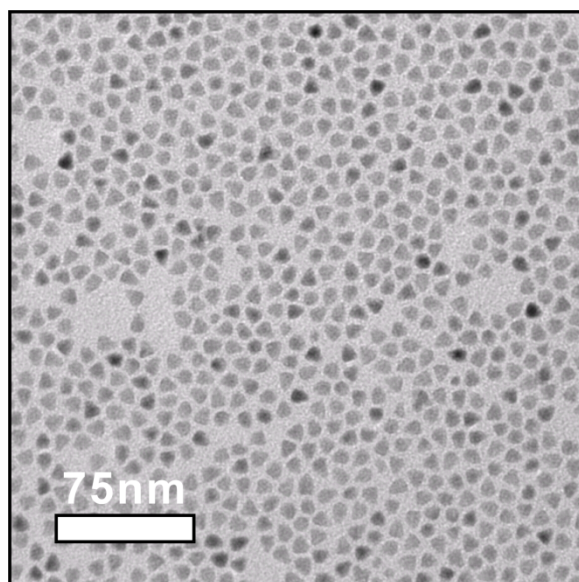


Figure S10. TEM image of CdSe/CdS core/shell QDs synthesized by the conventional method³. The average particle diameter is 9.0 nm with a relative standard deviation of $\pm 6\%$.

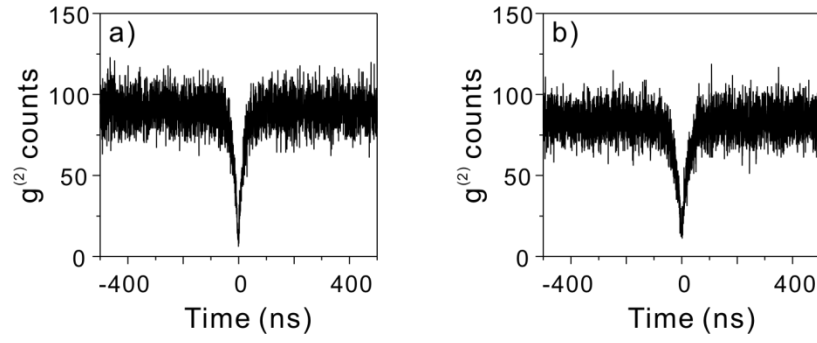


Figure S11. a) and b) are the $g^{(2)}(\tau)$ data of the same QDs of which blinking traces are shown in Figure 4a, d, respectively. It is clear that photons are strongly antibunched, confirming that the PL intensity traces (Figure 4a, d) were collected from single-QDs.

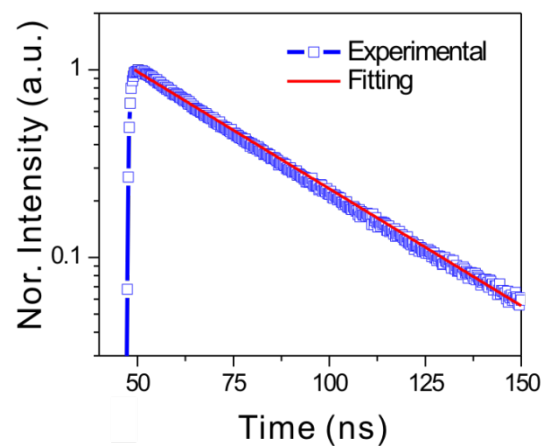


Figure S12. Ensemble PL decay of our new generation CdSe/CdS core/shell QDs. Red line is a monoexponential fit with a lifetime (τ) of ~ 32 ns.

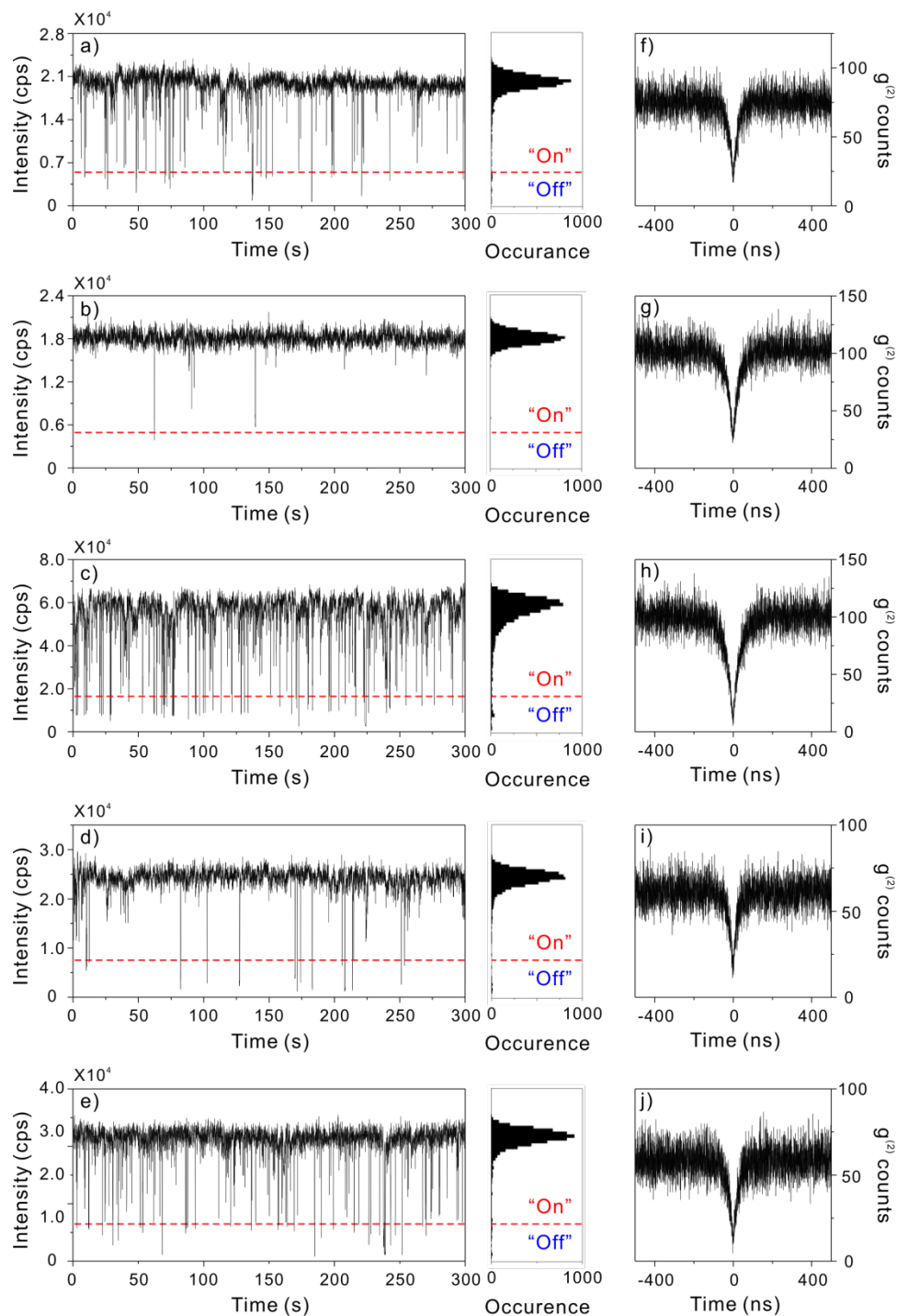


Figure S13. Representative blinking traces a)-e) and corresponding $g^{(2)}(\tau)$ measurements f)-j) of single-QDs from the samples of CdSe/CdS with a CdSe core diameter of 4.4nm and CdS shell thickness of 2.35 nm (~ 7 ML). Histograms indicate the distribution of intensities observed in the trace. The dashed red line indicates the value chosen as the threshold between "on" and "off" states.

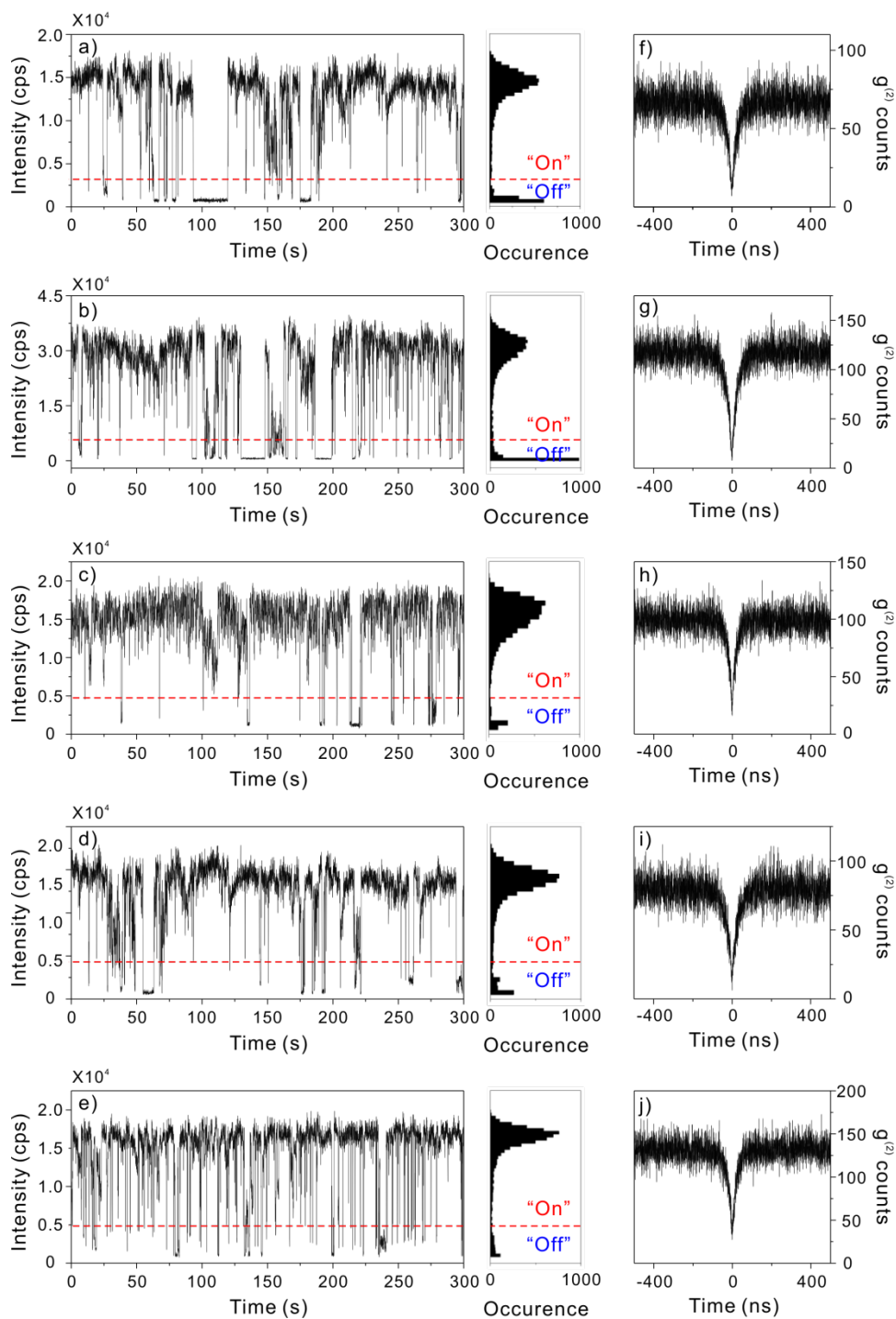


Figure S14. Representative blinking traces a)-e) and corresponding $g^{(2)}(\tau)$ measurements f)-j) of single QDs from the samples of CdSe/CdS with a CdSe core diameter of 4.4nm and CdS shell thickness of 0.7 nm (~2 ML). Histograms indicate the distribution of intensities observed in the trace. The dashed red line indicates the value chosen as the threshold between "on" and "off" states.

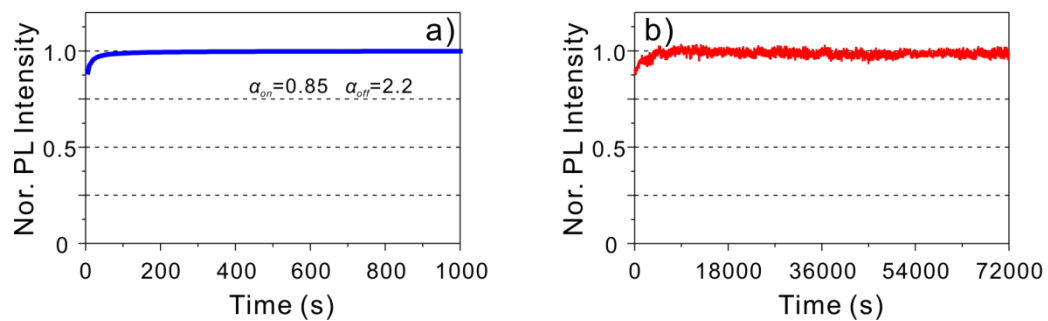


Figure S15. Evolution of the ensemble PL QY (the “on” fraction) as a function of time: a) calculation result; b) experimental data. The calculation result qualitatively fit the experimental data.

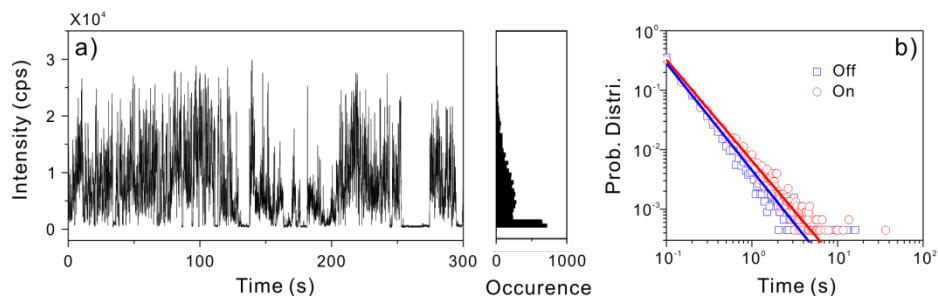


Figure S16. a) Representative single QD PL blinking trace with a bin size of 50 ms from the sample of CdSe/CdS core/shell QDs synthesized by the conventional method. Histograms indicate the distribution of intensities observed in the trace. b) Log-log plot of the probability of “on” and “off” events extracted from the single QD blinking traces of CdSe/CdS QDs synthesized through conventional method³. Straight lines represent a power-law fitting using the equation of $P_{on/off}(t_{on/off}) \propto t^{-\alpha_{on/off}}$ where both α_{on} for “on” times (red line) and α_{off} for “off” times (blue line) are ~ 1.7 . No upper bound cutoff time was observed for both “on” time and “off” time distributions within the time region of single QD measurements.

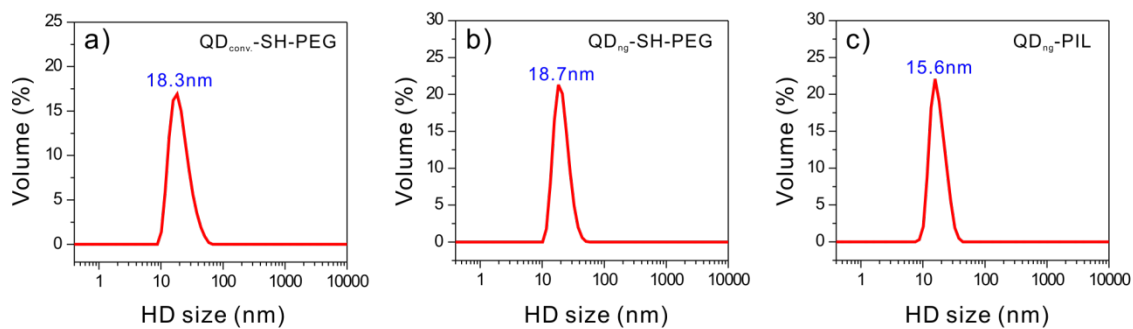


Figure S17. Dynamic light scattering (DLS) measurements of QDs dissolved in phosphate buffer saline solution (PBS 1X, pH 7.4) after ligand exchange. a) Methoxy-polyethylene-glycol thiol capped CdSe/CdS core/shell QDs synthesized by a conventional method³ (QD_{conv.}-SH-PEG), b) methoxy-polyethylene-glycol thiol (PEG-SH) capped new generation (ng) CdSe/CdS core/shell QDs synthesized by our new method (QD_{ng}-SH-PEG), c) polymeric imidazole ligands (PILs) capped new generation CdSe/CdS core/shell QDs synthesized by our novel method (QD_{ng}-PIL).

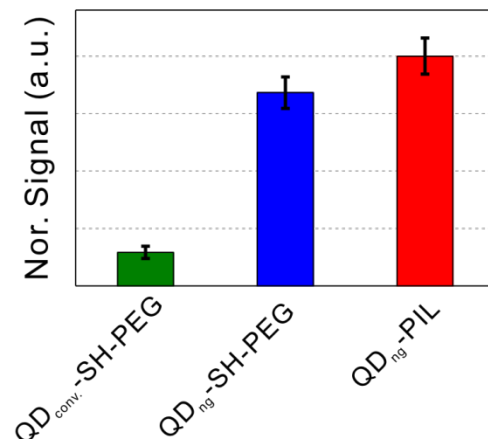


Figure S18. Normalized fluorescence signal intensity (Nor. Signal) inside blood vessel. Green: methoxy-polyethylene-glycol thiol capped conventional CdSe/CdS core/shell QDs synthesized by the literature method³ (QD_{conv.}-SH-PEG); Blue: methoxy-polyethylene-glycol thiol (PEG-SH) capped new generation (ng) CdSe/CdS core/shell QDs synthesized by our new method (QD_{ng}-SH-PEG); Red: polymeric imidazole ligands (PILs) capped new generation (ng) CdSe/CdS core/shell QDs synthesized by our new method (QD_{ng}-PIL).

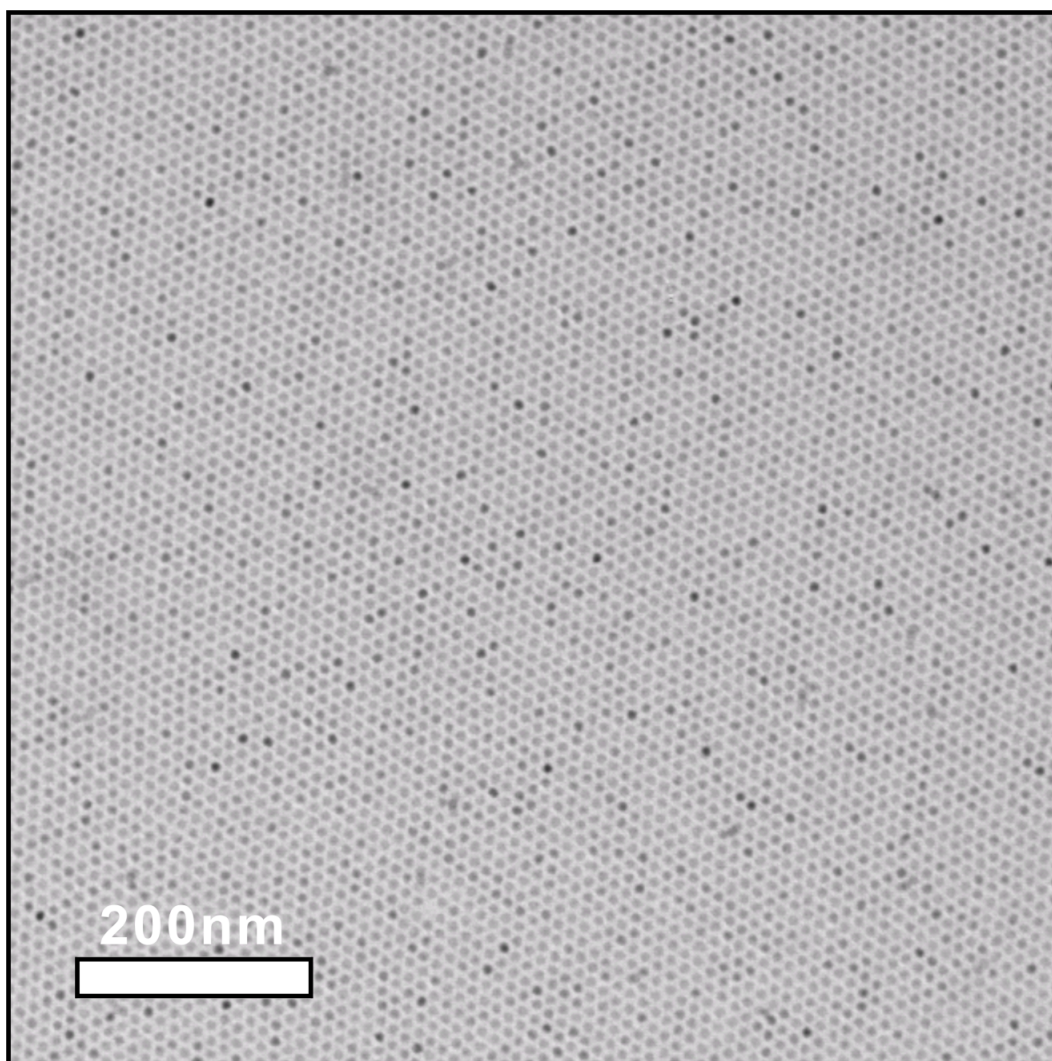


Figure S19. A large area TEM image of new generation CdSe/CdS core/shell QDs synthesized by our method with an average diameter of 8.2 nm (CdSe cores diameter of 4.2 nm, CdS shell thickness of 2.0 nm) and relative standard deviation of $\sim 3.9\%$.

References:

1. Carbone, L. et al. Synthesis and micrometer-scale assembly of colloidal CdSe/CdS nanorods prepared by a seeded growth approach. *Nano Lett* **7**, 2942-2950 (2007).
2. Chen, O. et al. Synthesis of metal-selenide nanocrystals using selenium dioxide as the selenium precursor. *Angew Chem Int Edit* **47**, 8638-8641 (2008).
3. Li, J.J. et al. Large-scale synthesis of nearly monodisperse CdSe/CdS core/shell nanocrystals using air-stable reagents via successive ion layer adsorption and reaction. *J Am Chem Soc* **125**, 12567-12575 (2003).
4. Liu, W. et al. Compact biocompatible quantum dots via RAFT-mediated synthesis of imidazole-based random copolymer ligand. *J Am Chem Soc* **132**, 472-483 (2010).
5. Marshall, L.F., Cui, J., Brokmann, X. & Bawendi, M.G. Extracting spectral dynamics from single chromophores in solution. *Phys Rev Lett* **105**, 053005 (2010).
6. Cui, J. et al. Direct probe of spectral inhomogeneity reveals synthetic tunability of single-nanocrystal spectral linewidths. *Submitted* (2012).
7. Zhao, J., Chen, O., Strasfeld, D.B. & Bawendi, M.G. Biexciton quantum yield heterogeneities in single CdSe (CdS) core (shell) nanocrystals and its correlation to exciton blinking. *Nano Lett* **12**, 4477-4483 (2012).
8. Live cell imaging: a laboratory manual. (Cold Spring Harbor Laboratory Press, NY; 2010).
9. Brown, E.B. et al. In vivo measurement of gene expression, angiogenesis and physiological function in tumors using multiphoton laser scanning microscopy. *Nat Med* **7**, 864-868 (2001).
10. Chauhan, V.P. et al. Fluorescent nanorods and nanospheres for real-time in vivo probing of nanoparticle shape-dependent tumor penetration. *Angew Chem Int Edit* **50**, 11417-11420 (2011).
11. Duda, D.G. et al. Differential transplantability of tumor-associated stromal cells. *Cancer Research* **64**, 5920-5924 (2004).